Int. J. Heat Mass Transfer. Vol. 27, No. 10, pp. 1701–1713, 1984
Printed in Great Britain

0017 9310/84 $3.00 + 0.00

Fluid-phase radial transport in packed beds of low tube-to-particle diameter ratio

ANTHONY G. DIXON, MICHAEL A. DiCOSTANZO* and BRIAN A. SOUCY†
Department of Chemical Engineering, Worcester Polytechnic Institute, Worcester, MA 01609, U.S.A.

(*Received* 16 *May* 1983 *and in revised form* 5 *December* 1983)

Abstract—Mass transfer experiments were carried out in packed beds of spheres of low tube-to-particle diameter ratio ($3 \leqslant d_t/d_p \leqslant 12$) to determine, by analogy, the fluid-phase contribution to the heat transfer effective radial Peclet number and the apparent wall Biot number. The asymptotic Peclet number was shown to be between 8 and 11 for the entire d_t/d_p range, contradicting standard correlations. A correlation for the wall Sherwood number is given that extends those of previous studies:

$$Sh_{wf} = (1.0 - 1.5(d_p/d_t)^{1.5})(Sc)^{1/3}(Re)^{0.59}.$$

These results are in good agreement with data obtained directly from heat transfer experiments.

INTRODUCTION

PACKED bed tubular reactors are widely used in the chemical processing industry to carry out solid-catalyzed reactions. Many of these catalytic reactions are strongly exothermic, necessitating heat removal, which is usually accomplished by means of a multitubular reactor in which long narrow tubes are immersed in a heat exchange medium. Such tubes may be many hundreds of particle diameters long, but only a few across, facilitating radial heat loss to the tube wall. Thus knowledge of the effective radial heat transfer mechanisms through the packing and the wall for fluid flowing through a single tube forms an important aspect of the design of catalytic reactors. The case of low tube-to-particle diameter ratio (d_t/d_p) is clearly particularly important.

Packed bed heat transfer studies use a pseudo-homogeneous two-dimensional (2-D) model, in which the bed is modelled as though it consisted of one phase only. This composite phase is assumed to move in plug flow, with the ρC_p of the fluid phase, but at a superficial velocity, v, obtained by dividing the fluid volumetric flow rate by the total bed cross-sectional area. Axial and radial conduction are both then superimposed on this flow, and the effective thermal conductivities, which are based here on total bed area, are usually taken to be independent of the axial and radial spatial coordinates. In non-adiabatic beds, an apparent wall heat transfer coefficient must then be introduced to account for the decrease in effective conductivity near the wall. The model parameters are obtained from steady-state temperature measurements in non-reacting beds, for which the model equations are, in dimensionless form [1, 2]

$$\frac{1}{Pe_r}\left(\frac{\partial^2\theta}{\partial y^2} + \frac{1}{y}\frac{\partial\theta}{\partial y}\right) + \frac{1}{Pe_a}\frac{\partial^2\theta}{\partial x^2} = \left(\frac{R}{d_p}\right)\frac{\partial\theta}{\partial x} \quad (1)$$

with boundary conditions

$$\text{at } y = 1 \qquad \frac{\partial\theta}{\partial y} + (Bi)\theta = \begin{cases} Bi & x > 0 \\ 0 & x < 0 \end{cases} \quad (2a)$$

$$\text{at } y = 0 \qquad \frac{\partial\theta}{\partial y} = 0 \quad (2b)$$

$$\text{at } x \to \infty \qquad \theta \to 1 \quad (2c)$$

$$\text{at } x \to -\infty \qquad \theta \to 0. \quad (2d)$$

In the short beds generally used for experimental studies, it is important to retain the term representing effective axial transport, so that estimates of the radial transport parameters, Pe_r and Bi, are not biased. In long industrial beds it is more important to have accurate values for Pe_r and Bi than the axial parameter, Pe_a.

Literature correlations of the radial parameters show considerable scatter, especially for the wall heat transfer coefficient [3]. In the face of such empirical results a more fundamental approach was adopted, namely to predict the effective parameters *a priori* from consideration of the underlying fluid and solid phase transport mechanisms [4].

The relationships obtained from this procedure were

$$\frac{1}{Pe_r} = \frac{1}{Pe_{rf}} + \frac{k_{rs}}{k_f}(Re\,Pr)^{-1}\left(\frac{Bi_f + 4}{Bi_f}\right)\left[\frac{8}{N_s} + \frac{Bi_s + 4}{Bi_s}\right]^{-1} \quad (3)$$

where

$$N_s = \frac{1.5(1-\varepsilon)(d_t/d_p)^2}{(k_{rs}/k_f)\{1/Nu_{fs} + 0.1/(k_p/k_f)\}} \quad (4)$$

* Present address: Union Oil, P.O. Box 76, Brea, CA 92621, U.S.A.

† Present address: Cabot Corporation, Billerica, MA 01821, U.S.A.

NOMENCLATURE

A	constant defined in equation (8)
b	constant defined in equations (17) and (18)
Bi	Biot number for heat, $h_w R/k_r$
Bi_m	Biot number for mass, $k_w R/D_r$
C	concentration of diffusing species [kg mol m^{-3}]
C_p	specific heat [kJ kg^{-1} K^{-1}]
D	diffusivity [m^2 s^{-1}]
d_t	tube diameter [m]
d_p	pellet diameter [m]
h	heat transfer coefficient [kW m^{-2} K^{-1}]
J_i	Bessel function of the ith order
k	thermal conductivity [kW m^{-1} K^{-1}]
k_w	wall mass transfer coefficient [kg mol m^{-2} s^{-1} (kg mol m^{-3})$^{-1}$]
N_s	defined in equation (4)
Nu	Nusselt number, hd_p/k_f
Pe	Peclet number, $\rho v C_p d_p/k$
$Pe(\infty)$	asymptotic value of Pe at large Re
Pr	Prandtl number, $\mu C_p/k_f$
R	bed radius [m]
Re	Reynolds number, $\rho v d_p/\mu$
Sc	Schmidt number, $\mu/\rho D_f$
Sh_{wf}	Sherwood number, $k_w d_p/D_f$
v	superficial fluid velocity [m s^{-1}]
x	dimensionless axial coordinate
y	dimensionless radial coordinate.

Greek symbols

β_n	defined below equation (10)
ε	bed voidage
θ	dimensionless temperature or concentration
$\bar{\theta}$	annular average θ
λ_n	eigenvalue defined in equation (11)
μ	viscosity of fluid [kg m^{-1} s^{-1}]
ρ	density of fluid [kg m^{-3}].

Subscripts

a	axial
c	center core
f	fluid
fs	fluid-to-solid
i	inner annulus
m	mass
o	outer annulus
p	pellet
r	radial
s	solid
w	wall
wf	wall-to-fluid

Note: All transport coefficients are based on unit void plus non-void area perpendicular to the transfer direction.

and

$$Bi(d_p/R) = Bi_f(d_p/R) = Nu_{wf}\frac{Pe_{rf}}{Re\ Pr}. \quad (5)$$

The predictions of Bi and Pe_r by equations (3)–(5) agreed well with valid experimental data, however, several of the individual-phase parameters had to be guessed or obtained by extrapolation of rather limited experimental data. This was especially the case for low d_t/d_p, where there were few studies, in spite of the practical importance of this area.

The determination of single-phase transport parameters is thus well motivated, not only by the above argument, but also by the increasing use of heterogeneous models in packed bed studies, as more complicated phenomena are studied. This also leads to a requirement of better accuracy in the parameters of even the simpler models.

The object of this study is to investigate transport through the fluid phase alone, and to provide correlations for Pe_{rf} and Nu_{wf} in terms of Re and d_t/d_p for ranges of low d_t/d_p. A companion study has also been carried out to clarify solid-phase heat transfer over similar ranges.

PREVIOUS WORK

It is desirable to obtain fluid-phase transport parameters from mass transfer experiments, in order to eliminate the contribution of the solid phase, which is always present in low d_t/d_p heat transfer studies under practical laboratory conditions. The heat transfer parameters are given by heat–mass analogies

$$Pe_{rf} = Pe_{rm} \quad (6)$$

and

$$\frac{Nu_{wf}}{Re\ Pr^{1/3}} \equiv j_H = j_D \equiv \frac{Sh_{wf}}{Re\ Sc^{1/3}}. \quad (7)$$

There have been few studies of the wall-to-fluid mass transfer coefficient made under conditions truly analogous to the case of heat transfer from the wall. One such study is that of Yagi and Wakao [5], who coated a tube with 2-naphthol, and then ran water through the packed column, dissolving the 2-naphthol from the walls. They measured only one item of data, the mixed-mean concentration, but required to estimate two parameters, Pe_{rm} and Sh_{wf}. They were therefore constrained to assume $Pe_{rm} = Pe_r$, available from separate heat transfer experiments. This is clearly not

the case except at high d_t/d_p and large flow rates, as shown by equations (3) and (4). Their experimental method, however, is sound and is the basis for the procedure followed in the present work.

Olbrich and Potter [6] measured the vaporization of mercury from the wall into a nitrogen stream. They had to consider also simultaneous axial and radial gas mixing in the voids as well as accounting for the pressure drop across the bed. They further used a non-standard estimation procedure which did not allow the determination of the wall mass transfer coefficient at individual Re values. Their results differ by an order of magnitude from those of other workers.

The remaining studies all used electrochemical techniques, in which limiting current measurements were made. The ferricyanide–ferrocyanide ion conversion system was often used, with electrodes located on the wall of the packed bed. A review of four such investigations has been given by Storck and Coeuret [7]. The correlations listed there may be rewritten in terms of Sh_{wf}, assuming $\varepsilon = 0.4$, and they are shown in Table 1. Also shown is a correlation of the results of Kunii and Suzuki [8], derived during the present work in order to represent their data for $Re > 2$ by a single equation.

The agreement between the different correlations is very good, however, these results were nearly all obtained for $d_t/d_p > 10$. Storck and Coeuret [7] interpret the wall mass transfer coefficient as an average representing the diffusional boundary layer. There is no *a priori* reason to expect the one-phase parameter, Sh_{wf}, to be well-predicted by these relations, as it is hard to say precisely what mechanisms contribute to Sh_{wf}.

Radial mixing experiments to determine Pe_{rm} have generally followed the lines of Fahien and Smith [9]. A stream of tracer gas was introduced into the bed via an injection pipe placed at the bed axis, and the resultant mixture analyzed at various positions in the bed downstream from the point of injection. Either point samples were withdrawn [9], or an annular arrangement was used to give averaged concentrations [10]. Analysis of the data has ranged from graphical differentiation to least-squares fitting. Most studies have produced Peclet numbers averaged over the bed radius although that of Fahien and Smith also gave point values. Fahien and Smith gave an expression for the dependence on (d_t/d_p) of $Pe_{rm}(\infty)$

$$Pe_{rm}(\infty) = A\{1 + 19.4(d_p/d_t)^2\} \tag{8}$$

where $8 \leqslant A \leqslant 10$, the form of which was supported by the work of Roemer *et al.* [11], and also by Olbrich and Potter [6], who took $A = 7$. It is, however, doubtful whether the (d_p/d_t) ratios used were severe enough to fully test the correlation.

However, these results are not strictly applicable to the case where a mass transfer analogue of Pe_{rf} is required. All studies except that of Olbrich and Potter used the wall boundary condition

$$\frac{\partial \theta}{\partial y} = 0 \text{ at } y = 1. \tag{9}$$

Table 1. Sh_{wf} correlations from electrochemical studies

Authors	d_t/d_p	Correlation
Krishna *et al.*	10–27	$Sh_{wf} = 0.82(Sc)^{1/3}(Re)^{0.62}$
Rao and Rao	—	$Sh_{wf} = 0.79(Sc)^{1/3}(Re)^{0.60}$
Smith and King	9.3–49	$Sh_{wf} = 0.90(Sc)^{1/3}(Re)^{0.62}$
Storck *et al.*	9.2–92	$Sh_{wf} = 0.86(Sc)^{1/3}(Re)^{0.61}$
Kunii and Suzuki*	2–100	$Sh_{wf} = 0.70(Sc)^{1/3}(Re)^{0.63}$

* Rectangular bed.

Therefore the radially-averaged Peclet numbers of such workers include mass transfer resistance all the way to the wall, whereas the extra resistance to radial mass transfer near the wall is covered by the use of the Sherwood number in the study of Olbrich and Potter, in the same way that extra resistance to radial heat transfer near the wall is covered by the use of the Nusselt number.

EXPERIMENTAL EQUIPMENT AND PROCEDURE

The objective of the experiments was to obtain mass transfer data under conditions as similar as possible to those used for temperature profiles, so that the parameters, Pe_{rm} and Sh_{wf}, could be determined and would represent the same fluid mixing mechanisms as in the heat transfer case.

The experimental approach was to pump water through a packed column, and to allow a soluble material to dissolve from the coated column walls into the stream, which was then sampled at the bed exit. This arrangement is shown schematically in Fig. 1.

The column was constructed in three sections from 3 in. I.D. copper tubing, with water-tight seals in the flanges between the sections. The water was introduced into a 6 in. uncoated packed calming section at the top of the assembly, through a center inlet port. A cap with four separate entry ports was also used for some experiments, to guard against channelling. As no difference in the results was observed between the two feed methods, it was concluded that the inlet water was well-distributed across the column. The middle section was the packed and coated test section. The length of the test section was varied between 6 and 12 in., to see if axial effects were important. The packing rested on a brass wire support grid at the bottom of this section. Details of the packing are given in Table 2, with

Table 2. Packing materials

Packing	d_t/d_p	ε
1/4 in. nylon spheres	11.8	0.42
5/16 in. nylon spheres	9.4	0.40
3/8 in. nylon spheres	7.8	0.40
1/2 in. nylon spheres	5.9	0.42
3/4 in. polystyrene spheres	3.9	0.47
1 in. nylon spheres	2.9	0.47

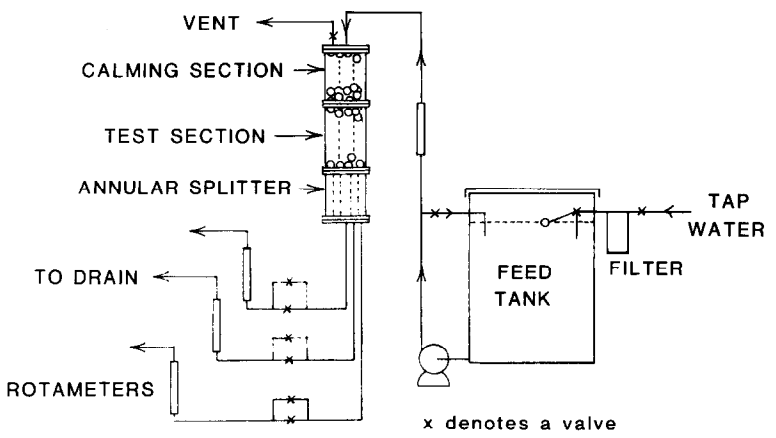

FIG. 1. Schematic description of mass transfer apparatus.

approximate voidages obtained by separate measurements of the volume of water in a packed test section. These voidages were reproducible to within ± 0.02. The final section of the column was a 6 in. long annular splitter, similar to that used by Gunn and Pryce [10]. This device contained concentric 1 and 2 in. I.D. tubes, allowing three annular radially-averaged samples to be obtained.

Two procedures were used for coating the test section of the column.

(1) A wooden handle was fastened to the tube flange, the entire test section was dipped into a tank of the molten coating material, then quickly transferred to an ice–water bath, to solidify the coating. Excess coating was removed from the outside of the tube, which was then bolted into place in the apparatus.

(2) Molten material was poured into the test section, which was then closed-off by endplates and hand-rotated until the material set.

The results showed no difference between setting in air or in water. Both methods gave a smooth, hard, even coating, with no cracks or pits visible. The materials used are discussed in the next section. The columns were checked after the runs, and no bare spots were observed. A slight pitting at points of contact between the packing and the tube wall was present. The coating was relatively thin, so that any change in thickness was negligible for these experiments.

With the coated section in place, the column was filled with water. Valves on the exit lines were then opened and closed in turn in a procedure designed to bleed the column of air. These valves were then used to control the flow rates through the annuli, i.e. to control the sampling rates. It was important to set these flow rates so that the presence of the annular splitter immediately below the packing support grid did not influence flow inside the bed. To do this it was necessary to know the velocity profile inside the bed in order to compute the flow rate through the corresponding annulus in the bed. Attempts to measure the radial velocity profile by pitot tubes failed as the radial pressure drop was of the same magnitude as system fluctuations. It was therefore necessary to assume a velocity profile (uniform) and adjust the annular flow rates accordingly. This point is discussed further in later sections, where other velocity profiles are considered. It should be noted that the same problem exists if point samples are withdrawn, instead of the average samples taken in this study.

The column was operated and exit samples monitored until steady-state was reached; this took 10–12 h for runs with 2-naphthol as the coating, 24 h for cinnamic acid, but only 15 min for benzoic acid, a more soluble material. Final samples were taken and the total flow to the column adjusted to a new value. For each packing size five flow rates were used to give Reynolds numbers in the range $50 \leqslant Re \leqslant 500$. Most runs were repeated at least once with a new coating, and the data analyzed simultaneously, so that the parameters given here represent averages over re-packed beds.

The concentrations of the samples were obtained by measuring absorbances with a u.v.-spectrophotometer at wavelengths of 273 nm (2-naphthol, cinnamic acid) and 271 nm (benzoic acid).

Solubility data and plots of Schmidt number, Sc, against temperature were derived from the results of previous workers [12–14].

COATING MATERIALS

Three coating materials were used in this work: 2-naphthol, cinnamic acid, and benzoic acid. Adipic acid was also tried but did not adhere to the test section.

The values of Pe_{rm} for benzoic acid were slightly higher than for the other coatings. The differences were only just significant compared to the variation arising from repacking, but they were consistent for all flow rates. There was an extremely large coating effect on Sh_{wf}, with benzoic acid results 2–3 times the cinnamic acid results and 3–7 times the 2-naphthol results. Only the benzoic acid results were of the same order of magnitude as the electro-chemical studies.

These coating effects are not new. Using the same

materials, Steele and Geankoplis [14] found three distinct lines for j_D vs Re in their study of mass transfer from spheres to water at high Re. Similarly Linton and Sherwood [13] found benzoic acid to give higher values than the other two materials in open-tube turbulent flow at $Re > 1000$. For mass transfer from solid shapes they again found benzoic acid to give higher results, agreeing more with vaporization studies.

Explanations of these effects have not been totally successful. Linton and Sherwood attributed their results to surface roughness and fissures for the open-tube runs, and reported a j_D–Re curve which resembled the friction-factor curve for roughened tubes. Inspection of our tubes after use revealed no differences between the coatings, however, even though there were large solubility differences. Steele and Geankoplis even artificially roughened a sphere, and saw no effect on the results. These latter workers also detected a mass flux even at zero driving force, which they felt was related to attrition of crystals, crystalline structure and the ability of the coatings to crystallize. They brought their results into agreement using pseudosolubility (i.e. pseudotemperature) at the wall for benzoic acid. Thus they increased the apparent driving force at the wall, which resulted in a reduced mass transfer coefficient and j_D-factor. It is hard to see any physical justification for such a procedure.

The key to these observations, however, does seem to lie with the materials' solubilities. If there were a decreased rate of dissolution, because wall solubility was less than expected, then the Sh_{wf} would be underestimated. This might occur, for example, if a surface contaminant were present. Some evidence to support this view comes from the work of Garner and Suckling [15] who studied flow around single spheres of benzoic acid and adipic acid. They found one correlation to be sufficient for both coatings, although adipic acid is five times as soluble as benzoic. Both are much more soluble than 2-naphthol or cinammic acid.

Our present conclusions are that it is not known why the differences between coatings occur, but that results from high-solubility coatings appear to be more reliable. The remainder of this study is therefore based only on results from benzoic acid coatings.

MATHEMATICAL TREATMENT

The material balance for the experimental column described above leads, as intended, to the same dimensionless equations as for the heat transfer case, equations (1) and (2), save only that the parameters, Pe_r, Bi, and Pe_a must be replaced by Pe_{rm}, Bi_m, and Pe_{am}, respectively. The infinite series solution to these equations is easily obtained by separation of variables [1] and is, for $x > 0$

$$\theta(x,y) = 1 - \sum_{n=1}^{\infty} \frac{Bi_m(1+\beta_n)J_0(\lambda_n y)}{(Bi_m^2+\lambda_n^2)\beta_n J_0(\lambda_n)} \times \exp\left(\frac{Pe_{am}}{2}\frac{R}{d_p}x(1-\beta_n)\right) \quad (10)$$

where

$$\beta_n = \sqrt{\left(1 + \frac{4\lambda_n^2}{Pe_{am}\,Pe_{rm}}\left(\frac{d_p}{R}\right)^2\right)}$$

and the λ_n are the roots of

$$\lambda_n J_1(\lambda_n) - Bi_m J_0(\lambda_n) = 0. \quad (11)$$

The case of negligible axial dispersion (plug flow) may be derived by allowing $Pe_{am} \to \infty$.

To analyze the data in this study, it is necessary to average equation (10) across a radial annulus. Following Gunn and Pryce [10] the average is defined in this case by

$$\bar{\theta}(x) = \frac{2}{(y_o^2 - y_i^2)}\int_{y_i}^{y_o}\left(\theta - \frac{d_p}{R}\frac{1}{Pe_{am}}\frac{\partial\theta}{\partial x}\right)y\,dy. \quad (12)$$

Performing the indicated integration gives, after some algebra

$$\bar{\theta}(x) = 1 - \frac{1}{(y_o^2-y_i^2)}\sum_{n=1}^{\infty} \times \left[\frac{Bi_m(1+\beta_n)^2(y_o J_1(\lambda_n y_o) - y_i J_1(\lambda_n y_i))}{\lambda_n(Bi_m^2+\lambda_n^2)\beta_n J_0(\lambda_n)} \times \exp\left(\frac{Pe_{am}(1-\beta_n)x}{2}\frac{R}{d_p}\right)\right]. \quad (13)$$

Letting $Pe_{am} \to \infty$ gives, for the plug-flow case

$$\bar{\theta}(x) = 1 - \frac{1}{(y_o^2-y_i^2)}\sum_{n=1}^{\infty} \times \left[\frac{4Bi_m(y_o J_1(\lambda_n y_o) - y_i J_1(\lambda_n y_i))}{\lambda_n(Bi_m^2+\lambda_n^2)J_0(\lambda_n)} \times \exp\left(-\frac{\lambda_n^2 x}{Pe_{rm}}\frac{d_p}{R}\right)\right]. \quad (14)$$

The data give three dimensionless annular averages for each run, and nearly all runs were repeated at least once. The parameters were estimated by minimizing the sum of squares of residuals (differences between observed and calculated values) using a finite-difference Levenberg–Marquardt algorithm. This method allowed the estimation of 95% confidence intervals for each parameter. The Sherwood number was obtained from the relation

$$(Bi_m)\left(\frac{d_p}{R}\right) = (Sh_{wf})\left(\frac{Pe_{rm}}{Re\,Sc}\right). \quad (15)$$

Initially equation (13) was fitted to data from several bed lengths simultaneously, at the same Re. The confidence intervals showed Bi_m and Pe_{rm} to be reasonably well determined, however, no reliable estimates of Pe_{am} could be obtained and the algorithm had difficulty converging. When equation (14) was fitted to data from single bed depths, it was observed that there were no axial trends in the residuals, and that the parameters, Pe_{rm} and Bi_m, showed no significant dependence on bed depth. It was therefore concluded that equation (14) provided an adequate fit to the data, and only two parameters were estimated in this study.

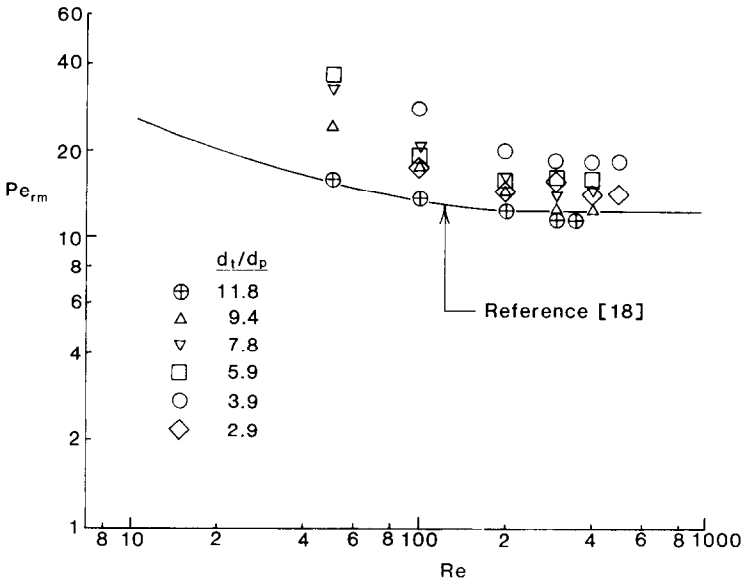

FIG. 2. Pe_{rm} from uniform velocity runs.

RESULTS USING UNIFORM VELOCITY PROFILES

The first set of data points was obtained with the sampling rates set under the assumption of a uniform velocity, i.e. independent of radial position. The fitted values of Pe_{rm} and Sh_{wf} are shown in Figs. 2 and 3, respectively, plotted against Reynolds number.

In Fig. 2 the values of Pe_{rm} decrease with Re to an asymptotic value, $Pe_{rm}(\infty)$, and are close to this value for $Re > 100$–200 approximately. This implies the existence of a maximum value for lower Re, which is in agreement with previous work [18]. An empirical correlating form, which allows representation of both of these features, can be derived from the diffusion–convection coupling theory of DeLigny [16]. The equation

$$\frac{1}{Pe_{rm}} = \frac{0.67\varepsilon}{Re\ Sc} + \frac{1/Pe_{rm}(\infty)}{(1+50/Re)} \tag{16}$$

fits the data with an average error of 15% of the experimental value. This equation can not be used to obtain Pe_{rm} values for gas mixing, as the relative magnitude of the diffusive and convective terms is very different from the liquid mixing case.

In Fig. 3 the Sh_{wf} values are given; these are well represented by an equation of the form

$$Sh_{wf} = b(Sc)^{1/3}(Re)^{0.59} \tag{17}$$

where b depends only on (d_t/d_p). The Re-dependence in this correlation is in excellent agreement with the

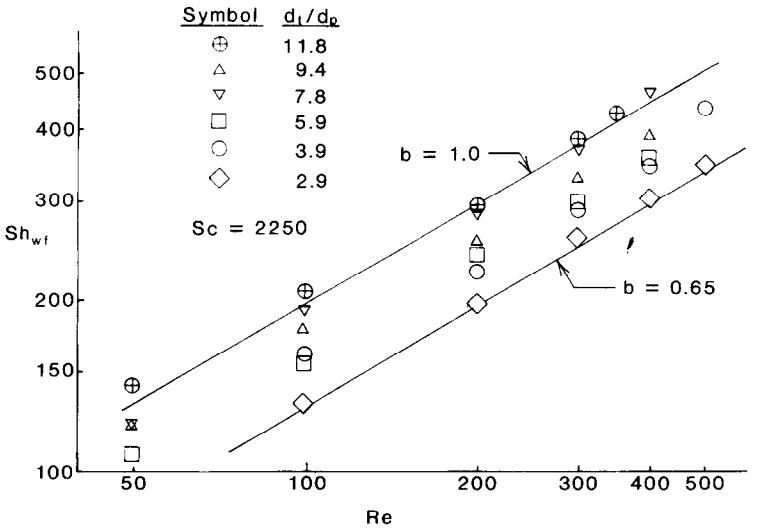

FIG. 3. Sh_{wf} from uniform velocity runs.

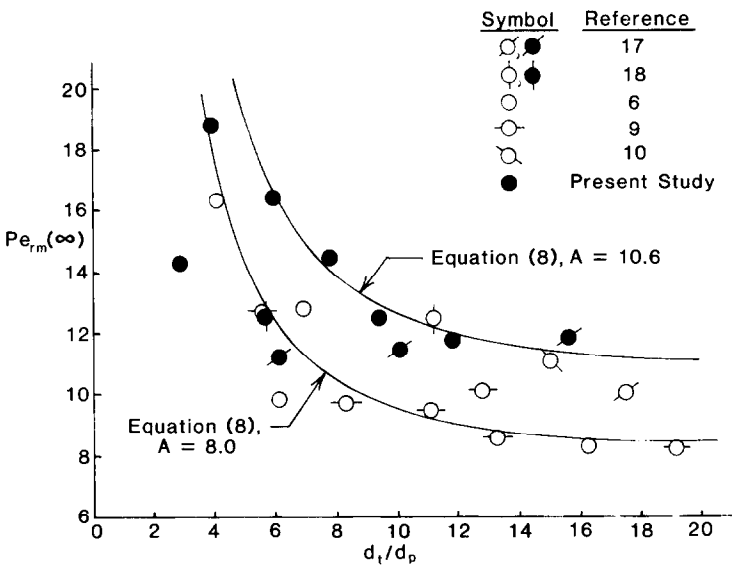

FIG. 4. Comparison of gas-phase (○) and liquid-phase (●) $Pe_{rm}(\infty)$ for spherical packing.

electrochemical studies presented earlier, and indicates that such studies do indeed yield Sh_{wf} values which are compatible with pseudohomogeneous models.

The effects of d_t/d_p in these equations are contained in the parameters b and $Pe_{rm}(\infty)$. Clearly Sh_{wf} increases as d_t/d_p increases over the range shown here, but the electrochemical studies at higher ratios show little effect over quite wide ranges. The two sets of results may be unified by the relation

$$b = (1.0\text{–}1.5(d_p/d_t)^{1.5}) \tag{18}$$

which is a reasonably simple empiricism.

Comparisons of $Pe_{rm}(\infty)$ as a function of d_t/d_p are made with previous studies in Fig. 4 and two versions of equation (8) are also shown. From these comparisons several observations may be made.

There is apparently no difference between 'average' $Pe_{rm}(\infty)$ values [9, 10, 17, 18] and 'bed-center' values [6] (also this study). This lack of distinction was not expected, however, it may be explained by considering the bed structure. For low d_t/d_p beds, Pe_{rm} varies with bed radius across the whole tube [9], as the voidage variations produced by the wall, extending about five particle diameters into the bed, are present everywhere when $d_t/d_p < 10$. In such cases only a small fraction of the wall effects can be accounted for by the localized wall mass transfer coefficient, in contrast to the high d_t/d_p case, where radial Pe_{rm} variation is confined to the near-wall region. It appears, therefore, that the use of Sh_{wf} does not affect an average Pe_{rm} significantly, and all experiments may be regarded as giving the same quantity.

It is also observed that $Pe_{rm}(\infty)$ is higher for liquid systems than for gas systems, in agreement with the conclusions of deLigny [16]. In the molecular diffusion and transition regimes of Pe_{rm} vs Re, it is not surprising that Pe_{rm} is higher for liquids, due to the much lower molecular diffusion coefficient as previously noted here and elsewhere [18]. In the fully turbulent regime, however, one would anticipate mixing in a packed bed to be the same for gases and reasonably-low-viscosity liquids at steady state, where no capacitative effect of stagnant films is possible.

Equation (8) represents the trends well for $d_t/d_p < 6$, however, for lower d_t/d_p the experimental points deviate seriously from this equation, for the results from the present study. This may be explained in a number of ways. First, it should be remembered that this equation is an empirical one, and it is probably not reasonable to expect that it should hold for $d_t/d_p < 6$, as Fahien and Smith [9] conducted no experiments in this region. Second is the likelihood that packed bed mixing changes dramatically and rapidly as d_t/d_p decreases through low values, for which the bed structure changes more radically as wall effects predominate than for variation of d_t/d_p over higher values. Finally is the probability that at low d_t/d_p the velocity profile becomes highly non-uniform, and thus the adjustment of sampling rates according to an assumption of uniformity may be inducing unwanted flow rearrangement effects within the bed.

RESULTS USING NON-UNIFORM VELOCITY PROFILES

To investigate the possibility that some of the observations noted above might be artifacts of the sampling procedure, the flow rates from the annuli were set according to non-uniform velocity profiles. This was the only change made from the previous experimental procedure and data analysis.

The first velocity profile used was the expression derived by Fahien and Stankovic [19] from the data of Schwartz and Smith [20], which has a maximum velocity one d_p from the wall. This expression was integrated over the annuli to give the three desired

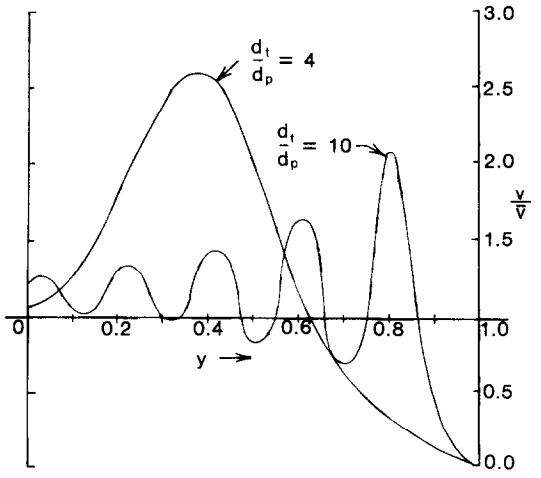

FIG. 5. Voidage-based velocity profiles.

volumetric flow rates. The experimental values of Pe_{rm} and Sh_{wf} obtained, however, showed almost no change from those in Figs. 2 and 3.

Some doubt has been cast upon whether velocity profiles measured above the packing truly represent those inside the bed [21, 22]. As all experimental velocity profiles have been obtained by such measurements, it is attractive to consider also a theoretical velocity profile, based on sound physical reasoning. A suitable expression has been developed by Cresswell [23], following the lines first suggested by Stanek and Szekely [24, 25]. The basis of the theory is the Ergun equation for pressure drop in a packed bed. Both velocity and voidage are allowed to vary in the radial direction; a formula for $\varepsilon(y)$ has been reported by Schlünder [26], in which $\varepsilon(y)$ undergoes damped oscillations from the tube wall to the bed center, of period close to d_p. The maxima and minima of velocity and voidage coincide, giving a very different velocity profile from that usually assumed. A problem arises at the wall, where voidage is at a maximum, however, the 'no-slip' boundary condition requires that velocity decrease to zero there. The Ergun equation is therefore applied only to a region $0 \leqslant y \leqslant y_c$, where y_c is an adjustable radial position, taken as a half particle diameter from the wall in the present study. In the near-wall region, the velocity is constrained to fall parabolically to zero from its value at $y = y_c$. Two profiles given by this voidage-based approach are shown in Fig. 5.

The experiments were repeated with the annular sampling rates obtained from integration of the voidage-based velocity profile. The parameters obtained are shown in Figs. 6 and 7, for comparison with the uniform velocity case.

For Sh_{wf} it can be seen that the values are a little higher than before, and the dependence on d_t/d_p has changed. The Re-dependence, however, is in agreement with equation (17) for $Re > 100$; at lower Re some deviation appears. The difference in magnitude can be explained by noting that the second set of runs were made at a lower water temperature, thus the Schmidt number was much higher in that case, increasing Sh_{wf}. The change in d_t/d_p-dependence is to be expected, as the velocity profile also depends on d_t/d_p, however, the data lie within the same limits on b as before.

The variation of Pe_{rm} with Re is again similar to that in Fig. 2, and the data may be correlated to an average error of less than 10% by the expression

$$\frac{1}{Pe_{rm}} = \frac{0.67\varepsilon}{Re\ Sc} + \frac{1/Pe_{rm}(\infty)}{(1+12/Re)} \tag{19}$$

which shows that the maximum in the curve is less pronounced than before.

The main difference between these results and those

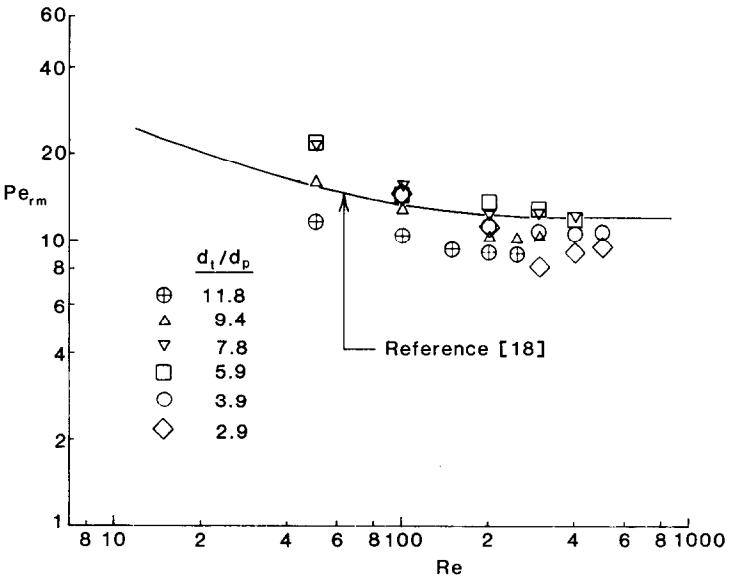

FIG. 6. Pe_{rm} from voidage-based velocity runs.

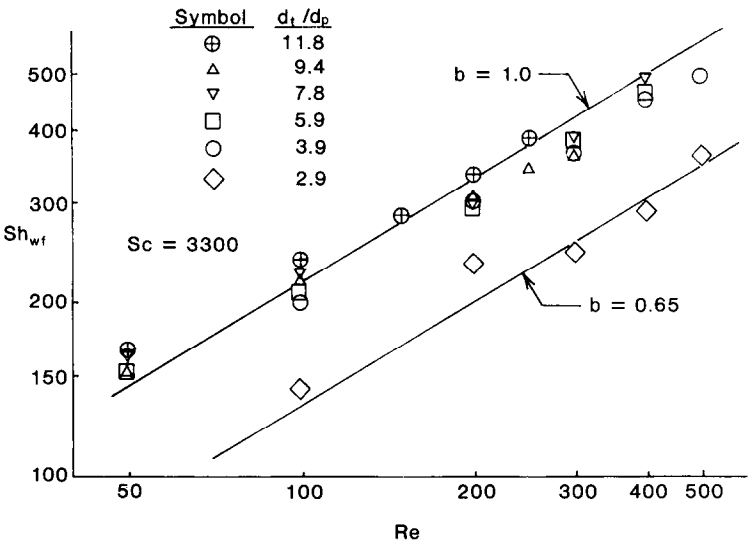

FIG. 7. Sh_{wf} from voidage-based velocity runs.

for uniform velocity sampling is in the d_t/d_p-dependence of $Pe_{rm}(\infty)$, given in Fig. 8. The values are now lower and lie closer to those obtained from the gas-phase studies [9], which used pitot tube sampling and a uniform velocity profile. Thus either pitot tube sampling is much less sensitive to the velocity profile assumed, or liquids and gases have quite different velocity profiles in packed beds. For $d_t/d_p \leqslant 6$ the results again show conclusively that equation (8) cannot safely be used outside the range for which it was derived.

The above discussion shows that it will be difficult to determine the d_t/d_p-dependence of $Pe_{rm}(\infty)$ until satisfactory velocity profiles are established for flow in packed beds. In the next section, however, the possibility of using heat transfer data directly is examined. This eliminates the sampling difficulties, but introduces other problems with the solid phase.

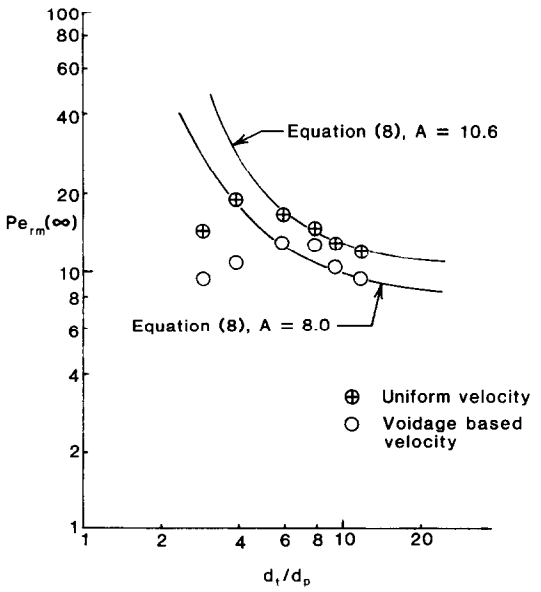

FIG. 8. $Pe_{rm}(\infty)$ from voidage-based velocity runs.

COMPARISON WITH HEAT TRANSFER RESULTS

It seems reasonable that if the solid-phase conductivity were well known, it would be possible to obtain the fluid-phase contribution to heat transfer directly from heat transfer data. A recent effort in this direction was that of Specchia *et al.* [27], who observed that the effective radial thermal conductivity varies linearly with Re for most of the published data. Treating the fluid and solid-phase contributions as being strictly additive, they obtained values of $Pe_{rf}(\infty)$ from the slopes of such plots, and confirmed equation (8) with $A = 8.65$ for a wide d_t/d_p range.

The difficulty with their method may be demonstrated by writing equation (3) in the form

$$\frac{k_r}{k_f} = \frac{1}{Pe_{rf}}(Re\,Pr) + \frac{k_{rs}}{k_f}\frac{(Bi_f+4)}{Bi_f}\left[\frac{8}{N_s} + \frac{Bi_s+4}{Bi_s}\right]^{-1} \tag{20}$$

and N_s is given by equation (4). It is clear that the slope of a plot of k_r/k_f against Re yields Pe_{rf} only if the second term on the RHS is constant. Unfortunately this term is flow-affected through Bi_f and N_s, which represent the influence of the tube wall and interphase heat transfer. This flow effect persists up to quite high Re; furthermore, it is not negligible when both phases are at the same temperature, as claimed by Specchia *et al.* [27], but only as $d_t/d_p \to \infty$, when wall effects also become negligible. Figure 9 shows a typical low d_t/d_p case with the two terms of equation (20) separately. Note that the flow-affected solid-phase term is linear for $Re > 100$ approximately.

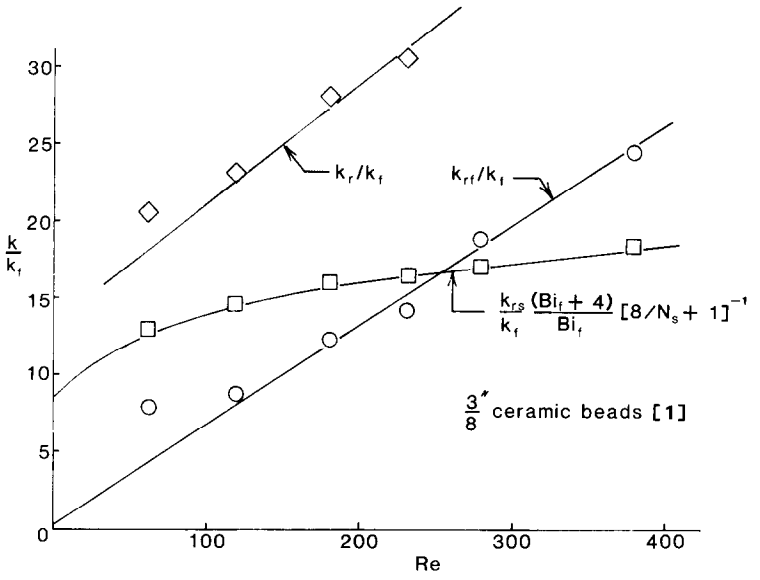

FIG. 9. Contributions to effective radial conductivity.

The simple method of Specchia *et al.* is thus seen to be correct only for large d_t/d_p studies. To obtain Pe_{rf} and Nu_{wf} from heat transfer studies, it is necessary to know k_{rs}/k_f, Bi_s, and N_s, and to solve equations (3)–(5) simultaneously for Pe_{rf} and Nu_{wf}, using experimental values of Pe_r and Bi. The fact that most studies report parameters which are bed-depth dependent, have been estimated by non-statistical methods, or which have been determined from unreliable experiments, has been discussed before [4] and severely limits the data base suitable for this procedure. Some limited results are shown in Fig. 10 for $Pe_{rf}(\infty)$; for the most part it was sufficient to take $Bi_s = \infty$ and $N_s = \infty$.

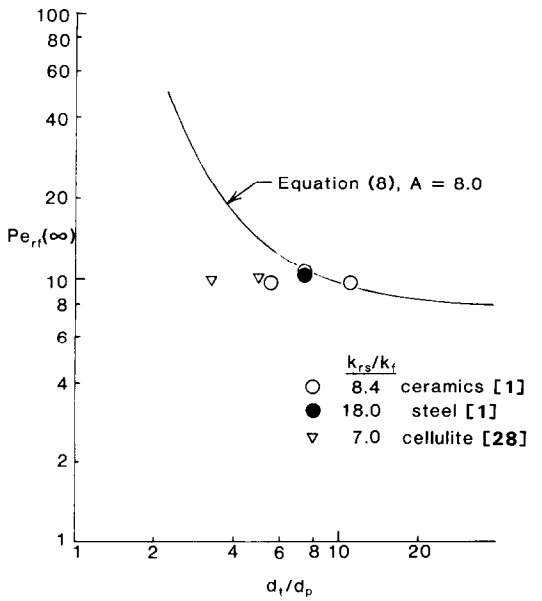

FIG. 10. $Pe_{rf}(\infty)$ from heat transfer studies.

Figure 10 shows that the $Pe_{rf}(\infty)$ from heat transfer studies are in good qualitative agreement with the $Pe_{rm}(\infty)$ from Fig. 8. This shows that $Pe_{rf}(\infty)$ remains fairly constant in the range 8–11, with $Pe_{rf}(\infty) = 10$ being a good average value for low d_t/d_p, while $Pe_{rf}(\infty) = 8$ may be more suitable as d_t/d_p increases.

The values of Nu_{wf} from this procedure confirm the correlations of equations (17) and (18), and are shown in Fig. 11. It is also instructive to examine the predictive ability of equations (3)–(5) with the new fluid-phase correlations. The value of $Pe_{rf}(\infty) = 10$ was suggested previously as a good average value, and led to good predictions of Pe_r [4]. An improved predictive formula for Bi can be given for $Re > 100$ as

$$Bi\left(\frac{d_p}{R}\right) = \left(1.0\text{–}1.5\left(\frac{d_p}{d_t}\right)^{1.5}\right)(Pr)^{-2/3} \times (Re)^{-0.41}(Pe_{rf}(\infty)) \quad (21)$$

where $8 < Pe_{rf}(\infty) < 10$. This is compared with data in Fig. 12, where the Re-dependence is well represented and much of the spread of the data accounted for. There is some deviation for lower Re values, which may be due to the omission of a solid-phase contribution in equation (5).

CONCLUSIONS

It is most important to know the velocity profile in a packed bed when carrying out mass transfer experiments at low d_t/d_p. Until this is established all studies of $Pe_{rm}(\infty)$ must be viewed with caution. In view of such uncertainty it is sufficient to regard $Pe_{rm}(\infty)$ as varying between 10 at low d_t/d_p and 8 at higher d_t/d_p. The popular formula of Fahien and Smith [9] has been shown to be unsafe for $d_t/d_p < 6$.

For Sh_{wf} a correlation has been found which agrees

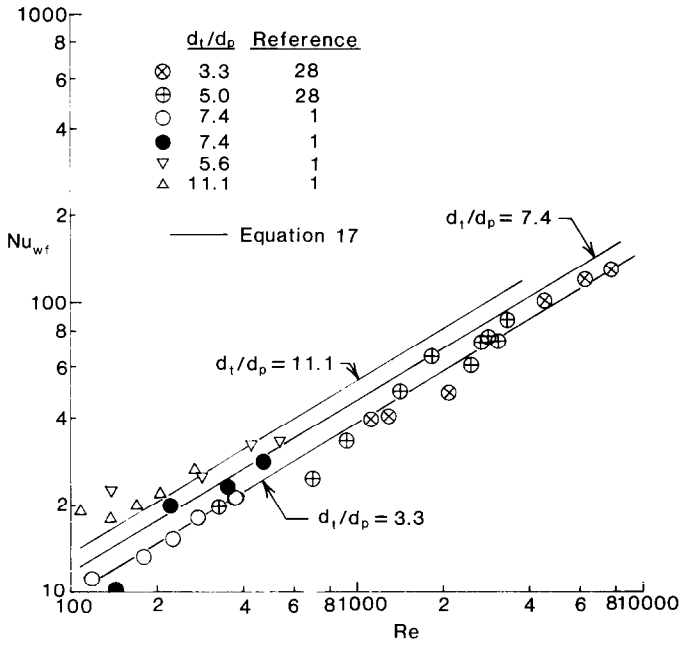

FIG. 11. Nu_{wf} from heat transfer studies.

with and extends the results of earlier electrochemical studies

$$Sh_{wf} = (1.0\text{–}1.5(d_p/d_t)^{1.5})(Sc)^{1/3}(Re)^{0.59}. \quad (22)$$

The effective radial heat transfer parameters are well predicted at higher Re by equations (3)–(5) using the above fluid-phase results. Some deviation at lower Re suggests that the solid-phase contribution may not yet be completely understood, especially for low d_t/d_p.

Acknowledgements—This material is based upon work supported by the National Science Foundation under Grant No. CPE-8106352. Thanks are also due to Worcester Polytechnic Institute for providing a research assistantship for Mr Soucy and Mr DiCostanzo, and to Dr David L. Cresswell for his valuable suggestions and advice.

REFERENCES

1. A. G. Dixon, D. L. Cresswell and W. R. Paterson, Heat transfer in packed beds of low tube/particle diameter ratio, *Chemical Reaction Engineering—Houston* (edited by V. W. Weekman and D. Luss), pp. 238–253. ACS Symp. Ser. No. 65 (1978).
2. D. J. Gunn and M. Khalid, Thermal dispersion and wall heat transfer in packed beds, *Chem. Engng Sci.* **30**, 261–267 (1975).
3. C.-H. Li and B. A. Finlayson, Heat transfer in packed beds—a reevaluation, *Chem. Engng Sci.* **32**, 1055–1066 (1977).
4. A. G. Dixon and D. L. Cresswell, Theoretical prediction of effective heat transfer parameters in packed beds, *A.I.Ch.E. Jl* **25**, 663–676 (1979).
5. S. Yagi and N. Wakao, Heat and mass transfer from wall to fluid in packed beds, *A.I.Ch.E. Jl* **5**, 79–85 (1959).
6. W. E. Olbrich and O. E. Potter, Mass transfer from the

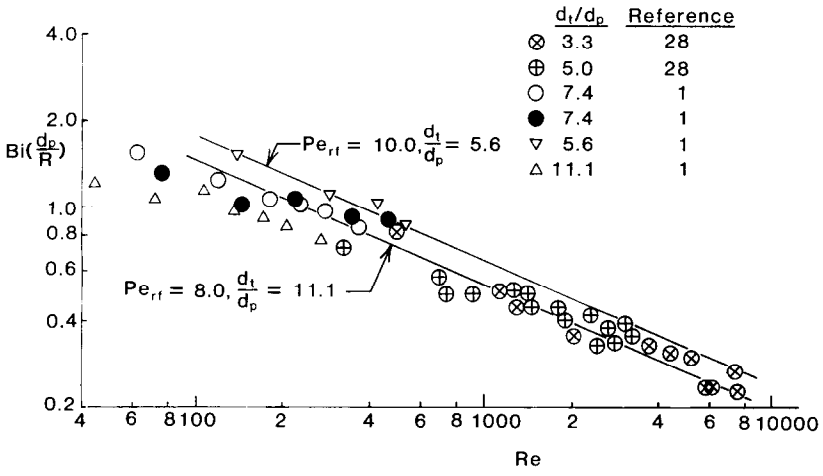

FIG. 12. Prediction of effective wall Biot number.

wall in small diameter packed beds, *Chem. Engng Sci.* **27,** 1733–1742 (1972).
7. A. Storck and F. Coeuret, Mass transfer between a flowing fluid and a wall or an immersed surface in fixed and fluidized beds, *Chem. Engng Jl* **20,** 149–156 (1980).
8. D. Kunii and M. Suzuki, Heat and mass transfer from wall surface to packed beds, *J. Fac. Engng Tokyo Univ.* **B30,** 1–15 (1969).
9. R. W. Fahien and J. M. Smith, Mass transfer in packed beds, *A.I.Ch.E. Jl* **1,** 28–37 (1955).
10. D. J. Gunn and C. Pryce, Dispersion in packed beds, *Trans. Instn. Chem. Engrs* **47,** T341–T350 (1969).
11. G. Roemer, J. S. Dranoff and J. M. Smith, Diffusion in packed beds at low flow rates, *Ind. Engng Chem. Fundam.* **1,** 284–287 (1962).
12. M. P. Moyle and M. Tyner, Solubility and diffusivity of 2-naphthol in water, *Ind. Engng Chem.* **45**(8), 1794–1797 (1953).
13. W. H. Linton and T. K. Sherwood, Mass transfer from solid shapes to water in streamline and turbulent flow, *Chem. Engng Prog.* **46,** 258–264 (1952).
14. L. R. Steele and C. J. Geankoplis, Mass transfer from a solid sphere to water in highly turbulent flow, *A.I.Ch.E. Jl* **5,** 178–181 (1959).
15. F. H. Garner and R. D. Suckling, Mass transfer from a solid sphere, *A.I.Ch.E. Jl* **4,** 114–124 (1958).
16. C. deLigny, Coupling between diffusion and convection in radial dispersion of matter by fluid flow through packed beds, *Chem. Engng Sci.* **25,** 1177–1181 (1970).
17. R. A. Bernard and R. H. Wilhelm, Turbulent diffusion in fixed beds of packed solids, *Chem. Engng Prog.* **46,** 233–244 (1950).
18. J. W. Hiby, Longitudinal and transverse mixing during single-phase flow through granular beds, *Instn Chem. Engrs Symp. Ser.* **9,** 312–325 (1962).
19. R. W. Fahien and I. M. Stankovic, An equation for the velocity profile in packed columns, *Chem. Engng Sci.* **34,** 1350–1354 (1979).
20. C. E. Schwartz and J. M. Smith, Flow distribution in packed beds, *Ind. Engng Chem.* **45**(6), 1209–1218 (1953).
21. J. J. Lerou and G. F. Froment, Velocity, temperature and conversion profiles in fixed bed catalytic reactors, *Chem. Engng Sci.* **32,** 853–861 (1977).
22. J. Schuster and D. Vortmeyer, Geschwindigkeitsverteilung in gas durchströmten, isothermen Kugelschüttungen, *Chemie-Ingr-Tech.* **53,** 806–807 (1981).
23. D. L. Cresswell, Personal communication to A. G. Dixon (1982).
24. V. Stanek and J. Szekely, The effect of non-uniform porosity in causing flow maldistribution in isothermal packed beds, *Can. J. Chem. Engng* **50,** 9–14 (1972).
25. V. Stanek and J. Szekely, Flow maldistribution in two dimensional packed beds part II: the behavior of non-isothermal systems. *Can. J. Chem. Engng* **51,** 22–30 (1973).
26. E. U. Schlünder, Transport phenomena in packed bed reactors, *Chemical Reaction Engineering Reviews—Houston* (edited by D. Luss and V. W. Weekman), pp. 110–161. ACS Symp. Ser. No. 72 (1978).
27. V. Specchia, G. Baldi and S. Sicardi, Heat transfer in packed bed reactors with one phase flow, *Chem. Engng Commun.* **4,** 361–380 (1980).
28. D. Kunii, M. Suzuki and N. Ono, Heat transfer from wall surface to packed beds at high Reynolds number, *J. Chem. Engng Japan* **1,** 21–26 (1968).

TRANSPORT RADIAL DE LA PHASE FLUIDE DANS LES LITS FIXES POUR UN FAIBLE RAPPORT DE DIAMETRES TUBE-PARTICULE

Résumé—Des expériences de transfert massique concernent des lits fixes de sphères avec un petit rapport de diamètres tube-particule ($3 \leqslant d_t/d_p \leqslant 12$) pour déterminer par analogie la contribution de la phase fluide dans le nombre de Péclet radial effectif et le nombre de Biot de paroi apparent. Le nombre de Péclet asymptotique est entre 8 et 11 pour le domaine entier de d_t/d_p, ce qui contredit les formules usuelles. Une formule pour le nombre de Sherwood est donnée qui étend les études antérieures:

$$Sh_{wf} = (1{,}0 - 1{,}5(d_p/d_t)^{1,5})(Sc)^{1/3}(Re)^{0,59}.$$

Ces résultats sont en bon accord avec les données obtenues directement à partir d'expériences de transfert thermique.

RADIALER TRANSPORT IN DER FLÜSSIGEN PHASE VON FESTBETTEN MIT KLEINEM VERHÄLTNIS VON ROHR- ZU PARTIKELDURCHMESSER

Zusammenfassung—Es wurden Versuche zum Stofftransport in Festbetten aus Kugelschüttungen mit kleinem Verhältnis von Rohr- zu Partikeldurchmesser ($3 \leqslant d_t/d_p \leqslant 12$) durchgeführt, um damit mit Hilfe der Analogie den Beitrag der Flüssigkeit zum effektiven radialen Wärmetransport zur entsprechenden Peclet-Zahl und zur scheinbaren Biot-Zahl der Wand zu bestimmen. Für den gesamten d_t/d_p-Bereich ergeben sich Werte für die asymptotische Peclet-Zahl zwischen 8 und 11, was den üblichen Gleichungen widerspricht. Es wird eine Korrelation für die Sherwood-Zahl der Wand angegeben, welche die Beziehungen aus vorangegangenen Untersuchungen erweitert

$$Sh_{wf} = (1{,}0 - 1{,}5(d_p/d_t)^{1,5})(Sc)^{1/3}(Re)^{0,59}$$

Diese Ergebnisse sind in guter Übereinstimmung mit Daten, die direkt aus Wärmeübergangsmessungen erhalten wurden.

РАДИАЛЬНЫЙ ПЕРЕНОС ЖИДКОЙ ФАЗЫ В ПЛОТНЫХ СЛОЯХ С НЕБОЛЬШИМ ОТНОШЕНИЕМ ДИАМЕТРА ТРУБЫ К ДИАМЕТРУ ЧАСТИЦ

Аннотация—Проведены эксперименты по массопереносу в плотных слоях сфер с малым отношением диаметров трубы и частиц ($3 \leq d_t/d_p \leq 12$) с целью определения по аналогии вклада жидкой фазы в эффективное радиальное число Пекле для теплопереноса и в истинное значение числа Био для стенки. Показано, что во всем исследованном диапазоне значений d_t/d_p асимптотическое число Пекле лежит в пределах 8–11, что противоречит результатам, получаемым по обычно используемым соотношениям. Выведена зависимость для числа Шервуда на стенке, которая обобщает и результаты ранее проведенных исследований:

$$Sh_{wf} = (1{,}0 - 1{,}5(d_p/d_t)^{1{,}5})(Sc)^{1/3}(Re)^{0{,}59}.$$

Результаты хорошо согласуются с данными, полученными непосредственно из экспериментов по теплопереносу.